Journal of Innovative Optical Health Sciences
Vol. 5, No. 3 (2012) 1250020 (5 pages)

DOI: 10.1142/S1793545812500204

INFLUENCE OF LIMITED-PROJECTION ON FLUORESCENCE MOLECULAR TOMOGRAPHY

YUN HE*, XU CAO*, FEI LIU*, JIANWEN LUO*,† and JING BAI*,‡
*Department of Biomedical Engineering, Tsinghua University
Beijing 100084, P. R. China
†Center for Biomedical Imaging Research, Tsinghua University
Beijing 100084, P. R. China
‡deabj@tsinghua.edu.cn

Accepted 23 June 2012
Published 2 August 2012

Challenges remain in imaging fast biological processes *in vivo* with fluorescence molecular tomography (FMT) due to the long data acquisition time. Data acquisition with limited projections can greatly reduce the time consumption, but the influence of limited-projection on reconstruction quality is currently unclear. Both numerical simulations and a phantom experiment are conducted to analyze this problem. Through a systematic investigation of all the results reconstructed from different numbers of projections, we evaluate the influence of limited-projection data on FMT. A mouse experiment is also performed to validate our work. A general relationship between the number of projections and reconstruction quality is obtained which indicates that the projection number of three is preferred for fast FMT experiment.

Keywords: FMT; inverse problem; limited-projection.

1. Introduction

Fluorescence molecular tomography (FMT) is a fast developing technology which is capable of high sensitively, noninvasively, quantitatively, and three-dimensionally imaging fluorescence markers attached to the designated molecules of small animals *in vivo*.[1] Therefore FMT has the potential of studying therapeutic response, disease pathogenesis, cancer diagnosis, and drug development in the ways of gene expression visualization, protein function determination, receptor localization, etc.[2]

The non-contact, free-space FMT with 360° angular projections was firstly introduced by Meyer *et al.* in 2007.[3] This system, in analogy to X-ray computed tomography, rotates the object imaged or the excitation and imaging device around the axis perpendicular to the camera's focal plane.[3,4] Thus it enables the 360° illumination and detection of the object instead of utilizing the inconvenient fiber-based system previously used.[5] With full projections of the photons emitting from all the surface of the object and an appropriate model of the photon propagation, the distribution of the inside fluorescent markers can be successfully reconstructed. Around 36−72 projections are generally captured to acquire the full dataset,[3,4,6−8] even more to achieve a higher resolution in reconstructed images.[9,10] In some of the recent reports, only 18−24 projections are collected in order to reduce computational or

‡Corresponding author.

experimental time cost.[11,12] Even so, the experimental procedure of acquiring the measurements consumes too much time, limiting its application in imaging some fast biological processes *in vivo*. FMT with fewer projections can lower the time consumption and be effectively adopted in such case only if it can still acquire enough information to retain a reliable reconstruction result.

In the following sections, this problem is analyzed by reconstructing fluorescent targets using a span of small projection numbers. The relationship between projection number and reconstruction quality is evaluated by a series of numerical simulations and a phantom experiment and further validated by a mouse experiment. The result suggests that FMT with three projections is feasible for fast imaging.

2. Method

In biological tissues, photon propagation can be modeled by the diffusion approximation to the radiative transport equation[13]

$$[\nabla D\nabla + \mu_a]U_m(\mathbf{r}) = -n(\mathbf{r})U_x(\mathbf{r}), \tag{1}$$

where $D = 1/3(\mu_a + \mu_s')$ is the diffusion coefficient; μ_a and μ_s' are possibly spatially varying absorption and reduced scattering coefficients; $U_x(\mathbf{r})$ and $U_m(\mathbf{r})$ denote photon density at excitation and fluorescence wavelength, respectively. $n(\mathbf{r}) = \eta(\mathbf{r})\mu_{af}$ is the fluorescent yield which is proportional to the concentration of fluorescent markers,[4] where η is the quantum efficiency of the fluorescent dye and μ_{af} is the fluorescent absorption coefficient.[14] If D and μ_a are known or estimated previously, the Green's function can be obtained by solving:

$$[\nabla D\nabla + \mu_a]G(\mathbf{r}, \mathbf{r}') = -\delta(\mathbf{r} - \mathbf{r}'). \tag{2}$$

We can rewrite Eq. (1) using Born approximation[15]:

$$U_m(\mathbf{r}) = \int_{\mathbf{r}'\in\Omega} G(\mathbf{r}, \mathbf{r}')n(\mathbf{r}')U_x(\mathbf{r}')d\mathbf{r}'. \tag{3}$$

Equation (3) can be linearly approximated by implementing the finite element method which discretizes the imaging domain Ω into a number of voxels.[16] Suppose that the imaging domain is discretized to N voxels and there are M detectors in one projection, the linear form of Eq. (3) is:

$$\begin{bmatrix} U_m(r_{d1}) \\ \vdots \\ U_m(r_{dM}) \end{bmatrix} = \begin{bmatrix} W_{11} & \cdots & W_{1N} \\ \vdots & \ddots & \vdots \\ W_{M1} & \cdots & W_{MN} \end{bmatrix} \begin{bmatrix} n(r_1) \\ \vdots \\ n(r_N) \end{bmatrix}. \tag{4}$$

Generally M is heavily smaller than N, which contributes to the underdetermination of this equation. It is also ill-posed due to photon propagation pattern inside biological tissues.[7] These two properties can greatly compromise the reconstruction quality especially when only a few projections are captured. Finally algebraic reconstruction technique is employed to solve the inverse problem.

3. Experiment

3.1. *Simulation study*

A series of numerical simulations were first conducted to systematically investigate this relationship between projection number and reconstruction quality. The object imaged was set to be a homogeneous cylinder with a radius of 1 cm and a height of 2 cm. The optical parameters were $\mu_a = 0.58\,\mathrm{cm}^{-1}$ and $\mu_s' = 10.0\,\mathrm{cm}^{-1}$. A number of smaller cylindrical fluorescent targets with a radius of 0.15 cm and a height of 0.3 cm were placed at the same height inside the object. The fluorescent yield n to be reconstructed was set as one. In an effort to have a general conclusion, three cases each with two, three, or four fluorescent targets were considered. Reconstructions were respectively carried out using a small number of projections varying from one to ten consecutively in each case. The position of the first projection was not specially chosen and remained the same in each reconstruction. Subsequent projections were captured in equal angle interval. 5% Gaussian white noise was deliberately added to all measurements to better approximate the experiment data. A commercial finite element method software COMSOL Multiphysics™ was employed to generate simulation data.

Figure 1 shows the cross sections of the reconstructed results at the center of the fluorescent targets. Similar tendencies can be found from all three cases. Results reconstructed from one or two projections fail to reveal the actual distribution of the fluorescent targets. However, images reconstructed from three projections show a marked improvement, which could locate the fluorescent targets correctly despite some quantification error. Results obtained from three to ten projections improve relatively much slowly compared with the ones from less than three.

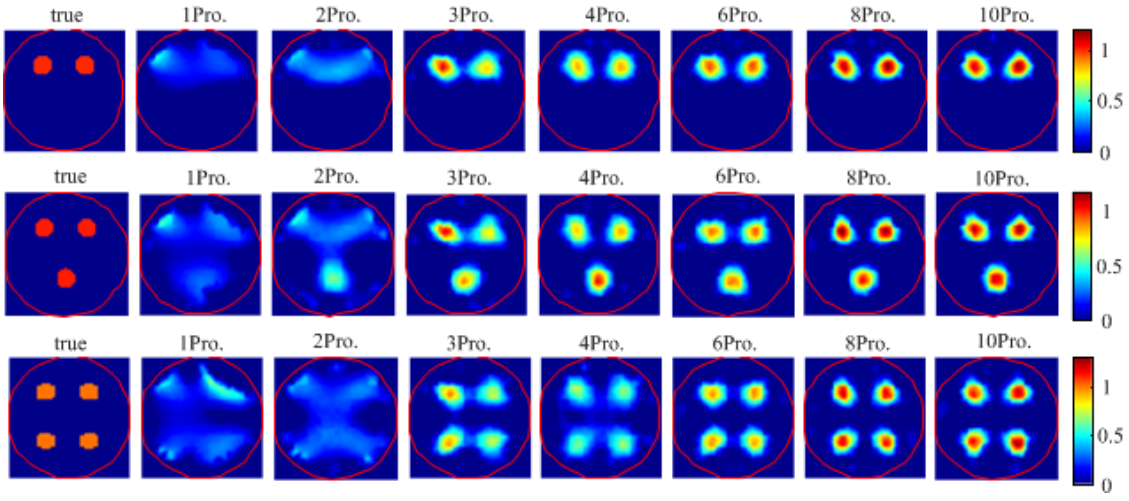

Fig. 1. Series of true and reconstructed images using different numbers of projections in all three cases.

In order to quantitatively describe the reconstruction quality, image quality index (IQI) is employed to evaluate all results.[17] The mathematical expression is given by:

$$\mathrm{IQI} = \frac{4\sigma_{xy}\bar{x}\bar{y}}{(\sigma_x^2 + \sigma_y^2)[(\bar{x})^2 + (\bar{y})^2]}, \tag{5}$$

where $\bar{x}$, $\bar{y}$, σ_x^2, and σ_y^2 denote the average value and variance of the true and reconstructed images, respectively. The IQI value as a function of projection number is shown in Fig. 2. All three curves follow a similar path. There is an initial steep increase up to three projections. However, only small improvement is gained with the further increasing number of projections. It appears that FMT with three projections is most preferred for fast data acquisition. We note that there are some ups and downs in the smooth part of the curve which are most likely caused by the ill-posedness of the inverse problem.

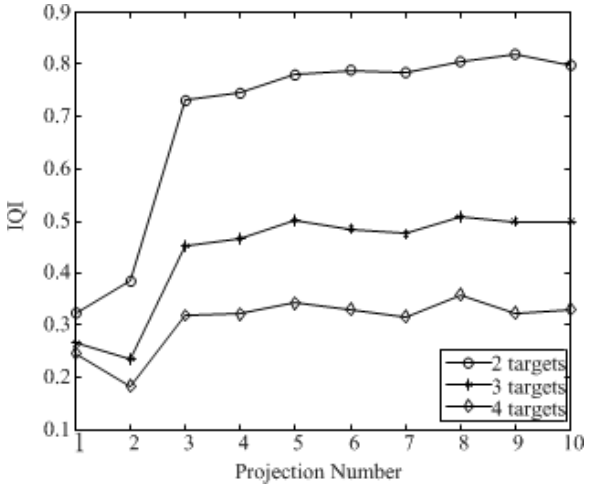

Fig. 2. IQI curves of all the reconstruction results in three cases.

3.2. *Phantom study*

A phantom experiment was also conducted to investigate this issue. A transparent glass cylinder (2.4 cm in diameter, 6.5 cm in height) filled with 1% intralipid was used as the phantom. The background optical properties are $\mu_a = 0.02\,\mathrm{cm}^{-1}$ and $\mu_s' = 10.0\,\mathrm{cm}^{-1}$. Two smaller transparent tubes (0.3 cm in diameter) filled with 10 μL Indocyanine Green (ICG) with a concentration of 1.3 μM were placed at the same height inside the phantom as the fluorescent targets. All experiments were conducted in a homemade FMT system which utilized a vertical line-shaped parallel excitation source for simultaneous whole-body imaging.[6] The line source was uniformly distributed along its length. About 36 angular projections in 10° steps were acquired as the full dataset. As the positions of the fluorescent targets were unknown, the position of first projection was not specially chosen. About 200 detectors are extracted from the surface in a field of view (FOV) of 170° and a height of 3.5 cm. The layout of the sources and detectors is depicted in Fig. 3, taking three projections for example.

Reconstructions were respectively conducted using a portion of the full dataset as the complete measurement and the position of the first projection was unchanged. Results reconstructed from

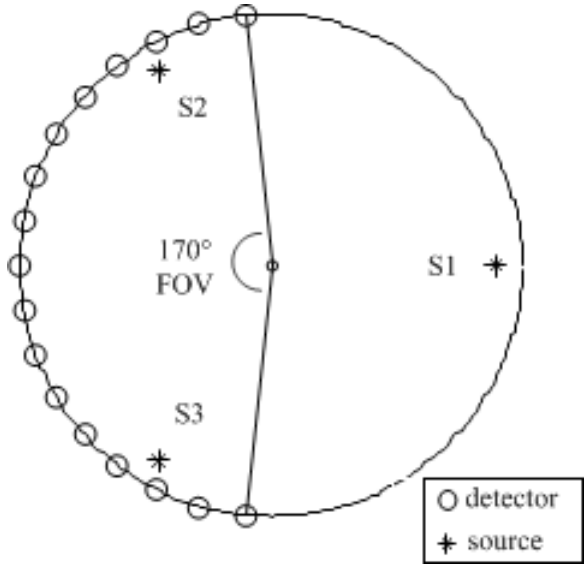

Fig. 3. Top view of the distribution of detectors and sources when capturing three projections. The asterisk S1 denotes the position of the line source in the first projection. And the small circles distributed in a 170° FOV with equal angular interval indicate detectors corresponding to S1. The asterisks S2 and S2 represent the source positions in the second and third projection, respectively.

different numbers of projections are demonstrated in Fig. 4. It can be seen that the tendency of the reconstruction quality resembles the IQI curve obtained in the simulation study. The result obtained with three projections depicts a significant improvement. However, the image quality improvement is relatively smaller as the projection number increases from four to 12. The IQI analysis is also conducted and demonstrated in Fig. 5. It can be seen that the result obtained in phantom study is in accordance with that in numerical simulations.

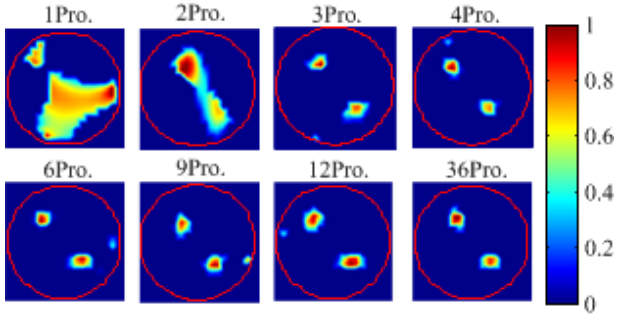

Fig. 4. Reconstruction results of the phantom study obtained with different numbers of projections. They are normalized by their respective maximum value.

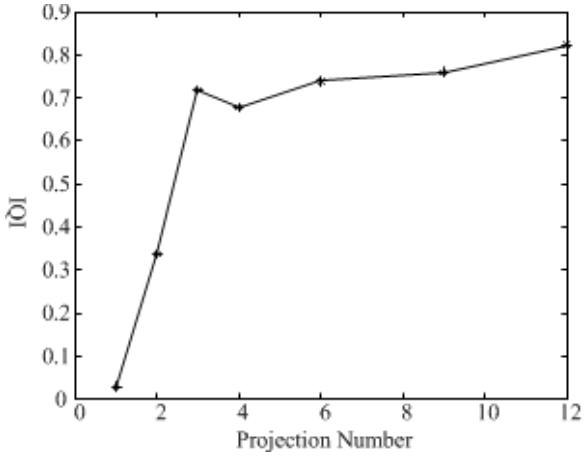

Fig. 5. IQI curve of the phantom experiment.

3.3. *Animal experiment*

Next, a mouse experiment was conducted to validate the performance of limited-projection FMT. A nude mouse was anesthetized and a transparent tube (0.4 cm in the outer diameter) filled with 1.3 μM ICG solution was implanted into the mouse from the anus as the fluorescent target. 24 projections were captured in equal angle interval.

The distribution of sources and detectors is similar to that in the phantom study except that the FOV is adjusted to 150° due to light leakage on the edge of the mouse. The position of the line source utilized in the first projection is also illustrated in Fig. 6(a). Optical parameters $\mu_a = 0.3\,\mathrm{cm}^{-1}$ and $\mu_s' = 10.0\,\mathrm{cm}^{-1}$ are employed in the reconstruction scheme. Results reconstructed from three and 24 projections are demonstrated in Figs. 6(b) and 6(c). They are normalized by their respective maximum value. The reconstruction results obtained from three projections match well with that obtained from 24 projections.

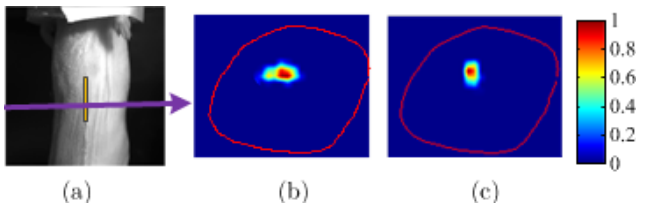

Fig. 6. Reconstruction results of mouse experiment obtained with different number of projections. (a) Position of the line source in the first projection is indicated by the yellow line. The arrow denotes the height of the two slices on the right. (b) and (c) The cross sections of the result reconstructed with three and 24 projections, respectively.

4. Conclusion

In this paper, a series of numerical simulations and a phantom experiment were conducted to evaluate the relationship between the projection number and the reconstruction quality in FMT when only a few projections are collected. Both results suggest that three projections are able to acquire the basic information of the fluorescent targets and yield a reliable reconstruction result. And only small improvement can be yielded by further increasing the number of projections. The performance of reconstruction with three projections is also verified by a mouse experiment. In conclusion, limited-projection FMT with more than or equal to three projections is capable of reducing experimental time consumption and retaining acceptable reconstruction quality, and the projection number of three is preferable for imaging fast biological processes *in vivo*.

Acknowledgments

This work is supported by the National Basic Research Program of China (973) under Grant No. 2011CB707701; National Major Scientific Instrument and Equipment Development Project (2011YQ030114); the National Natural Science Foundation of China under Grant No. 81071191, 60831003, 30930092, 30872633; the Beijing Natural Science Foundation Grant No. 3111003; the Tsinghua-Yue-Yuen Medical Science Foundation.

References

1. V. Ntziachristos, J. Ripoll, L. H. Wang, R. Weissleder, "Looking and listening to light: The evolution of whole-body photonic imaging," *Nat. Biotechnol.* **23**, 313 (2005).
2. V. Ntziachristos, "Going deeper than microscopy: The optical imaging frontier in biology," *Nat. Meth.* **7**, 603 (2010).
3. H. Meyer, A. Garofaiakis, G. Zacharakis, S. Psycharakis, C. Mamalaki, D. Kioussis, E. N. Economou, V. Ntziachristos, J. Ripoll, "Noncontact optical imaging in mice with full angular coverage and automatic surface extraction," *App. Opt.* **46**, 3617 (2007).
4. X. L. Song, D. F. Wang, N. G. Chen, J. Bai, H. Wang, "Reconstruction for free-space fluorescence tomography using a novel hybrid adaptive finite element algorithm," *Opt. Express* **15**, 18300 (2007).
5. V. Ntziachristos, C. Bremer, R. Weissleder, "Fluorescence imaging with near-infrared light: New technological advances that enable *in vivo* molecular imaging," *Eur. Radiology* **13**, 195 (2003).
6. F. Liu, X. Liu, D. F. Wang, B. Zhang, J. Bai, "A parallel excitation based fluorescence molecular tomography system for whole-body simultaneous imaging of small animals," *Ann. Biomed. Engrg.* **38**, 3440 (2010).
7. N. Deliolanis, T. Lasser, D. Hyde, A. Soubret, J. Ripool, V. Ntziachristos, "Free-space fluorescence molecular tomography utilizing 360 degrees geometry projections," *Opt. Lett.* **32**, 382 (2007).
8. D. F. Wang, X. Liu, Y. P. Chen, J. Bai, "*In vivo* fluorescence molecular tomography based on optimal small animal surface reconstruction," *Chin. Opt. Lett.* **8**, 82 (2010).
9. C. Vinegoni, D. Razansky, J. Figueiredo, M. Nahrendorf, V. Ntziachristos, R. Weissleder, "Normalized Born ratio for fluorescence optical projection tomography," *Opt. Lett.* **34**, 319 (2009).
10. H. Gang, J. Yao, J. Bai, "Full-angle optical imaging of near-infrared fluorescent probes implanted in small animals," *Prog. Natl. Sci.* **18**, 707 (2008).
11. T. Pyka, R. Schulz, A. Ale, V. Ntziachristos, "Revisiting the normalized Born approximation: Effects of scattering," *Opt. Lett.* **36**, 4329 (2011).
12. R. Schulz, A. Ale, A. Sarantopoulos, M. Freyer, E. Soehngen, M. Zientkowska, V. Ntziachristos, "Hybrid system for simultaneous fluorescence and X-ray computed tomography," *IEEE Trans. Med. Imaging* **29**, 465 (2010).
13. J. Ripoll, R. B. Schulz, V. Ntziachristos, "Free-space propagation of diffuse light: Theory and experiments," *Phys. Rev. Lett.* **91**, 103901 (2003).
14. X. Cong, W. Ge. "A finite-element-based reconstruction method for fluorescence tomography," *Opt. Express* **13**, 9847 (2005).
15. A. Soubret, J. Ripoll, V. Ntziachristos, "Accuracy of fluorescent tomography in the presence of heterogeneities: Study of the normalized Born ratio," *IEEE Trans. Med. Imaging* **24**, 1377 (2005).
16. D. F. Wang, X. L. Song, B. Jing, "Adaptive mesh based algorithm for fluorescence molecular tomography using an analytical solution," *Opt. Express* **15**, 9722 (2007).
17. Z. Wang, A. Bovik, "A universal image quality index," *IEEE Signal Proc. Lett.* **9**, 81 (2002).